HHS Public Access

Author manuscript

Cell Calcium. Author manuscript; available in PMC 2022 June 01.

Published in final edited form as:

Cell Calcium. 2021 June ; 96: 102380. doi:10.1016/j.ceca.2021.102380.

Two-photon calcium imaging of seizures in awake, head-fixed mice

Ala Somarowthu[a], **Kevin M. Goff**[b,c], **Ethan M. Goldberg**[a,c,d,e,*]

[a]Division of Neurology, The Children's Hospital of Philadelphia, Philadelphia, PA, 19104 U.S.A.

[b]Medical Scientist Training Program (MSTP), The University of Pennsylvania Perelman School of Medicine, Philadelphia, PA, 19104, U.S.A.

[c]The Neuroscience Graduate Group, The University of Pennsylvania Perelman School of Medicine, Philadelphia, PA, 19104, U.S.A.

[d]Department of Neurology, The University of Pennsylvania Perelman School of Medicine, Philadelphia, PA, 19104 U.S.A.

[e]Department of Neuroscience, The University of Pennsylvania Perelman School of Medicine, Philadelphia, PA, 19104 U.S.A.

Abstract

Epilepsy is a severe neurological disorder defined by spontaneous seizures. Current treatment options fail in a large proportion of patients, while questions as to the basic mechanisms of seizure initiation and propagation remain. Advances in imaging of seizures in experimental model systems could lead to a better understanding of mechanisms of seizures and epilepsy. Recent studies have used two-photon calcium imaging (2P imaging) in awake, behaving mice in head-fixed preparations to image seizures *in vivo* at high speed and cellular-level resolution to identify key seizure-related cell classes. Here, we discuss such advances and present 2P imaging data of excitatory neurons and defined subsets of cerebral cortex GABAergic inhibitory interneurons during naturalistic seizures in a mouse model of Dravet syndrome (*Scn1a*+/− mice) along with other behavioral measures. Results demonstrate differential recruitment of discrete interneuron subclasses, which could inform mechanisms of seizure generation and propagation in Dravet syndrome and other epilepsies.

*Corresponding author at: The Children's Hospital of Philadelphia, Abramson Pediatric Research Center, Room 502A, 3615 Civic Center Boulevard, Philadelphia, PA, 19104 U.S.A. goldberge@email.chop.edu (E.M. Goldberg).

Authors Contribution

Ala Somarowthu – Software; Validation; Formal analysis; Investigation; Data curation; Writing – Original Draft; Writing – Review & Editing.

Kevin M. Goff – Software; Validation; Formal analysis; Investigation; Data Curation; Writing – Review & Editing; Visualization.

Ethan M. Goldberg – Conceptualization; Methodology; Investigation; Writing – Original Draft; Writing – Review & Editing; Supervision; Project administration; Funding acquisition.

Declaration of Competing Interest

Declarations of interest: none.

Graphical Abstract

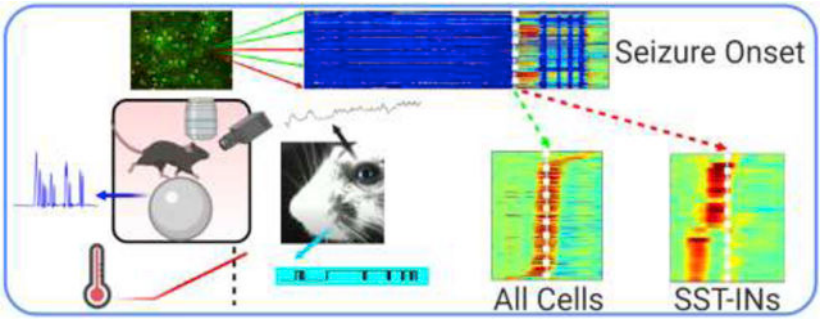

Created with BioRender.com

Keywords

Epilepsy; two-photon calcium imaging; Dravet syndrome

1. Introduction

Epilepsy is a neurological disorder defined by spontaneous unprovoked seizures and affects approximately 4% of the population at some point in their lifetime. The mechanistic basis of seizure initiation and propagation remains unknown despite decades of investigation but is thought to involve episodes of hypersynchronous neural activity across brain networks. However, epilepsy is not a singular disease but rather is composed of multiple syndromes of various etiologies that are linked by the presence of seizures. Broadly speaking, epilepsies can be acquired (secondary to, for example, traumatic brain injury or infection) or genetic (due to a highly penetrant dominantly acting pathogenic variant leading to epileptic encephalopathy, or due to complex polygenetic inheritance as in the more mild familial epilepsies). That seizures remain resistant to treatment in 30–40% of cases may relate to ongoing lack of understanding of basic mechanisms of seizure initiation and propagation, which may prove critical to inform the development of improved therapies or cure.

Prior work investigating mechanisms of seizures has focused on the role of defined neuronal classes – including excitatory and inhibitory neurons – in seizure initiation and propagation. Cerebral cortex neurons are divided into excitatory principal cells (PCs; including pyramidal cells and spiny stellate cells) and interneurons (INs); INs release the neurotransmitter GABA and mediate synaptic inhibition in the brain. Such neurons exhibit extensive within-class diversity [1,2], and are broadly divided into the following subclasses: parvalbumin (PV) immunoreactive fast-spiking basket cell INs (PV-INs) which form perisomatic and axo-axonic synapses and regulate action potential generation by target cells; somatostatin (SST) expressing dendrite-targeting Ins (SST-INs) that impinge on dendrites and regulate synaptic integration by target principal cells; and INs expressing vasoactive intestinal peptide (VIP-INs) which preferentially target SST-INs and are thought to subserve a largely disinhibitory role in cerebral cortex circuits [3–6]. In particular, PV-INs, the activity of which are known to regulate oscillations and rhythmogenesis [7–9], are thought to be critically important for

stabilizing cerebral cortex circuits, while disruption of PV-IN function leads to seizures and epilepsy [10]. An extensive literature including studies employing the *in vitro* acute brain slice technique [11–15] or work from intact experimental animals *in vivo* [16–19] supports the concept that seizure initiation involves dynamic imbalances between synaptic excitation and inhibition, which, while likely an oversimplification, has been a useful conceptual paradigm to model how circuit disruption can lead to seizures and epilepsy.

The standard tool used for recording and classifying seizures has been electroencephalography (EEG). But EEG lacks spatial resolution and cannot easily disentangle the relative contributions of neuron subclasses (or even neurons vs. glia) and instead is thought to reflect summated synaptic potentials involving thousands or millions of neurons [20]. Microelectrode arrays can resolve individual cell activity [21–23] but also lack the ability to readily identify cell type and cannot record a high density of neurons within a given brain area (although this field is also advancing rapidly; [24,25]).

Hence a role for two-photon (2P) laser scanning microscopic calcium imaging (2P imaging) which has emerged as a powerful tool for the potential study of seizures and epilepsy, based on the capacity of this technique for large-scale recording of neural activity *in vivo* and ready applicability to the study of local and global mechanisms of cerebral cortex circuit operations in experimental model systems, thereby bridging the gap between neuron-level and whole-brain activity in preclinical models of epilepsy [26]. In recent studies, 2P imaging and electrophysiology were combined to record chemically-induced seizure-like events and naturalistic seizures in anesthetized [16,17,27] and awake [19,27] mice.

Wenzel et al. (2017, 2019) [16,17] used 2P imaging along with LFP recording to study the dynamic progression of seizure-like events initiated using focal application of the chemoconvulsants 4-aminopyridine (4-AP) or picrotoxin in normal (non-epileptic) mice, and imaged the recruitment patterns of cell classes – including PCs and PV-INs – across layers. One advantage of this approach is that the putative seizure onset zone can be experimentally controlled. This approach also generates a focal event that does not progress to a generalized convulsive tonic-clonic seizure as is typical of many models of epilepsy in rodents, such as models of chronic acquired temporal lobe epilepsy after chemoconvulsant-induced status epilepticus. It is difficult or impossible to maintain a stable imaging plane during the sometimes violent movements associated with such seizures; Muldoon et al. (2015) [28] focused on interictal discharges (that are not associated with motor movement) for this reason. By controlling the site of the seizure initiation site, Wenzel et al. (2017, 2019) [16,17] showed that events start as hypersynchronous activation of local excitatory neuronal ensembles at the initiation site and invade smoothly into neighboring neocortex. In contrast, PV-INs show spatially non-uniform activity during initiation and propagation. Similar results were obtained in awake animals and anesthetized animals. However, questions remain as to how these findings might generalize to the mechanism of spontaneous seizure initiation and propagation in an epileptic animal [29].

Aeed et al. (2020) [18] studied the network mechanisms of chemically-induced seizure-like events provoked by focal application of 4-AP using 2P imaging along with electrophysiology in anesthetized and awake mice. The group used various IN-specific Cre

driver lines to study major subclasses of neocortical INs (PV and SST) along with PCs. Implementation of a prism [30] facilitated the simultaneous imaging of defined cell subclasses along the depth of the neocortex from layer 2/3 to 5. This study found that the activity of PCs and PV-INs in layer 2/3 and 4 was synchronous during spikes and seizure-like events; in contrast, layer 5 PCs and SST-INs were recruited gradually during seizure. While the activity of PCs and INs was shown to be balanced during spikes, there was an imbalance between activity of PCs and INs in layer 2/3 at seizure onset. These findings suggest a potential mechanistic relationship between spikes and seizures, with synchronous activation of layer 2/3 PCs in the context of PC:IN imbalance leading to or allowing transition from spike to seizure.

Genetic models of epilepsy have certain advantages for the study of seizures and epilepsy in experimental animals in a head-fixed preparation *in vivo*. Such models may yield spontaneous seizures or seizures that can be readily induced by physiologically relevant triggers, without the need for a chemoconvulsant agent that produces a seizure-like event typically via excitotoxicity, a block of $GABA_A$ receptors, blockade of potassium channels, or related mechanism that compromise or alter the normal physiology of cerebral cortex neurons. Spontaneously epileptic mice can be generated via breeding, rather than via induction protocols that can be laborious and ineffcient. Finally, genetic models may have absence seizures (characterized by arrest of activity; such as the stargazer mouse, or myoclonic (rapid jerks), or hemiclonic seizures (unilateral clonic activity) as in the Dravet syndrome (*Scn1a*+/−) mouse (see below), and such seizure types are more amenable to stable long-term 2P recording versus generalized convulsive tonic-clonic seizures.

Yet, few studies have employed 2P imaging towards the study of spontaneous or naturalistic seizures in epileptic mice *in vivo*. Meyer et al. (2018) [27] used 2P imaging along with electrophysiology to record absence seizures from awake stargazer mice (which have a spontaneously-occurring disruption in the calcium channel subunit *Cacng*). This genetic mouse model of absence epilepsy replicates key features of this common pediatric epilepsy syndrome. Individual visual neocortex (V1) neurons and surrounding neuropil showed reduced activity during seizures, while lower pairwise correlation between individual neurons implied decreased synchrony during seizures. These results suggest asynchronous suppression of neural activity in V1 during absence seizures, which was unexpected and illustrated the potential power of *in vivo* 2P imaging to reveal previously unknown features of seizures. This basic imaging approach was not applied to other brain regions to determine if the result obtains across neocortical areas beyond V1, as might be expected for a generalized epilepsy. This question could be approached using larger-scale imaging approaches (see Discussion).

In a previous paper from our group [19], we employed 2P imaging to record the activity of putative PCs and PV-INs during temperature-induced seizures in awake, behaving, head-fixed *Scn1a*+/− mice, a well-validated mouse model of a genetic epileptic encephalopathy known as Dravet syndrome (DS). DS is a neurodevelopmental disorder defined by treatment-resistant epilepsy with onset in the first year of life, temperature-sensitive seizures, moderate to severe developmental delay and intellectual impairment, and features of autism spectrum disorder, along with a high rate of seizure-related death, and is due to heterozygous

pathogenic loss-of-function variants in the gene *SCN1A* encoding the neuronal voltage-gated sodium channel subunit Nav1.1. As the most common type of so-called epileptic encephalopathy (severe epilepsy associated with developmental delay), DS affects 1 in 15,700 live births [31].

Accumulated evidence indicates that Nav1.1 is preferentially expressed in cerebral cortex INs and, in particular, in PV-INs, dysfunction of which has previously been idenfied in various experimental models of DS [32–37]. However, no data existed as to the activity of defined subsets of neurons in awake *Scn1a*+/− mice *in vivo*. We were particularly interested in the activity of these PV-INs along with putative PCs at transition to seizure. Such a study was facilitated by the fact that *Scn1a*+/− mice, much like human patients with Dravet syndrome, exhibit temperature-sensitive seizures, which can be readily induced in the laboratory. We generated a custom laser-cut temperature-controlled enclosure for manipulation of core body temperature that was compatible with a spherical treadmill apparatus upon which the experimental animal was able to rest or run during *in vivo* 2P imaging [19]. Cells were imaged using a genetically encoded calcium indicator, GCamp6f, introduced via stereotaxic injection of adeno-associated viral vectors, while PV-INs were labeled with tdTomato in *Scn1a*.PV-Cre.tdTomato mice.

We imaged PV-INs and putative PCs at baseline during quiet wakefulness and then during the preictal period leading up to seizure. Synchronization, bursting, and deconvolved relative firing rates were extracted from the individual cell-specific 2P imaging data. During quiet wakefulness at baseline, the activity of putative PCs and PV-INs was found to be higher in *Scn1a*+/− mice relative to wild-type. In the pre-ictal stage, PV-INs exhibited a gradual decrease in synchronization in *Scn1a*+/− mice. In WT mice, the same increase in core body temperature produced an increase in synchronization between PV-INs as well as between PV-INs and excitatory cells. These findings point to a preictal failure of PV-IN synchronization pre-seizure that may normally act to stabilize cerebral cortex circuits. A key feature of this study was the investigation of a naturalistic seizure (induced by an increase in body temperature, which in this case is a physiologically-relevant and model-specific seizure trigger) in the brain of an awake, behaving epileptic animal *in vivo.*

Here, we extend our prevous findings to study the activity of the three key subclasses of GABAergic INs, investigating the recruitment dynamics of PV-INs along with SST-INs and VIP-INs as well as putative PCs during temperature-induced seizures in *Scn1a*+/− mice. This study was further motivated by the finding that the electrical excitability of VIP-INs is also prominently impaired in *Scn1a*+/− mice *in vitro* [38]. Results presented here demonstrate differential recruitment of INs subclasses that may relate to the mechanisms of seizure generation and propagation.

2. Materials and methods

2.1. Experimental animals:

Three groups of mice (*Scn1a*.PV-Cre, SST-Cre, and VIP-Cre) were tested. All the procedures were approved by the Institutional Animal Care and Use Committee at The Children's Hospital of Philadelphia. All mice were heterozygous *Scn1a*+/− on a 50:50

C57BL/6J:129S6 mixed background as previously detailed [19,37,38], which is known to recapitulate the core features of Dravet syndrome as observed in humans. Mouse strains used included: *Scn1a*+/− mice on a 129S6.SvEvTac background (RRID:MMRRC_037107-JAX) generated by a targeted deletion of exon 1 of the *Scn1a* gene; PV-Cre mice (B6;129P2-Pvalbtm1(cre)Arbr/J; RRID:IMSR_JAX:008069); SST-IRES-Cre mice (RRID:IMSR_JAX:013044); VIP-IRES-Cre mice (IMSR_JAX:010908); wild-type 129S6.SvEvTac (Taconic Biosciences model #129SVE; RRID:IMSR_TAC: 129sve); tdTomato reporter Ai14 mice (Rosa- CAG-LSL-tdTomato; RRID:IMSR_JAX:007914; on a C57BL/6J background); and wild-type C57BL/6J (RRID:IMSR_JAX:000664). Heterozygous IN-Cre mice were crossed with homozygous Ai14 mice to generate double heterozygous IN-Cre.TdTomato mice, which were then crossed to *Scn1a*+/− mice to generate triple heterozygous *Scn1a*.IN-Cre mice and age-matched WT.IN-Cre littermate controls. Data from six *Scn1a*.PV-Cre.TdT, 4 *Scn1a*.VIP-Cre.TdT and 2 *Scn1a*.SST-Cre.Tdtomato mice were included for analysis.

2.2. Animal surgery:

Surgery was performed on mice age 6–10 weeks in the chronic phase of the disorder. Dexamethasone (5 mg/kg) was administered via intraperitoneal injection 4–6 hours prior to surgery. Mice were anesthetized by inhalation of isoflurane in oxygen (4–5% for induction, 0.8–2% for maintenance, in 0.5 L/min oxygen). Buprenorphine-SR (0.5–1.0 mg/kg) was injected (subcutaneously) immediately before surgery to reduce pain; cefazolin 500 mg/kg was injected subcutaneously for anti-bacterial prophylaxis. A three mm craniotomy was performed at the identified target area with a hand-held drill, and a bone flap was removed to expose the dura, which was removed using a microprobe. AAV9.hSyn.GCaMP6f.WPRE or AAV9.hSyn.GCaMP7s.WPRE was injected (20–40 nL) at 2–4 sites separated by 300–500 μm. A three mm diameter glass coverslip attached to a 5 mm glass coverslip via optical glue to create a “plug” that was inserted into the craniotomy and cemented to the skull along with a stainless steel head plate using cyanoacrylate glue covered with dental cement (Metabond).

2.3. Imaging:

2P imaging was performed on head-fixed awake mice using a customized Bruker 2P laser scanning microscope equipped with a mode-locked pulsed infrared laser (InSight, SpectraPhysics) controlled by a Pockels cell (Conoptics). Images were acquired at 30 Hz with a resonant scanner (Cambridge Technology), 16X/0.8-NA water immersion objective (Nikon), gallium arsenide phosphide (GaAsP) photodetector (H7422-40; Hamamatsu), and multi-alkali detector (R3896; Hamamatsu). Running speed and video of facial features (including pupil size and whiskers) were simultaneously recorded.

2.4. Data Analysis:

The collected 2P imaging data was analyzed using the Suite2p package in Python [39] to detect individual cells, extract fluorescence traces, and remove neuropil contamination of the signal. After subtracting the neuropil from these raw traces, the relative change in fluorescence dF/F_0 was computed for each cell. Ictal recruitment lags were calculated using the first derivative (slope) of the $dF/F0$ traces [17]. The slope (i.e., rate of change in $dF/F0$) was estimated using sliding window regression and the time point at which the $dF/F0$ trace

for an individual cell reached a maximum slope was considered as the recruitment time point for that cell. The 20-second window around seizure onset was retrieved for all seizures and grouped together for analysis. The differences in the recruitment were investigated by 1) comparing individual recruitment lags with seizure onset and 2) comparing the recruitment strength that is maximum dF/F_0 values in between the PCs and INs.

To analyze the behavioral data, we integrated running speed, pupil diameter, and whisker position. Points of interest around the pupil and on whiskers were recorded (Point Grey) and tracked using the DeepLabCut package [40]. A circle was fitted with the tracked pupil coordinates to derive pupil diameter. From the derived points of interest on the whiskers, the whisker movement was gated as “on” and “off” based on thresholding.

Group statistics were derived using linear mixed modeling by considering seizure number and mouse as random factors. Group means standard errors and significance (*p*-values) were derived from this mixed model. All the post-processing programs and statistics codes were written in MATLAB.

3. Results

3.1. Behavioral activity during temperature-induced seizures in Scn1a+/− mice:

We recorded core body temperature, locomotion, pupillometry, and whisking, simultaneous with 2P imaging of identified IN subtypes and putative PCs in a head-fixed preparation, during temperature-induced seizures in *Scn1a*.IN-Cre mice. An example of an imaging session depicting the various monitored parameters is shown in Fig. 1. We employed this paradigm to determine IN-specific activity and correlate it with various behavioral measures during the preictal period.

3.2. Recruitment dynamics of INs during a temperature-induced seizure:

Our prior work [19] investigated the activity of PV-INs and PCs during the pre-ictal phase and demonstrated preictal failure of PV-INs synchronization. We were interested in the activity of the other two major subclasses of cerebral cortex INs, SST- and VIP-INs, which was achieved by crossing *Scn1a*+/− mice to SST-Cre.tdTomato and VIP-Cre.tdTomato double transgenic mice.

We examined the raw $dF/F0$ traces (Panels A and C in Fig. 2, Fig. 3, and Fig. 4) and slope of the $dF/F0$ traces (Panels B and D in Fig. 2, Fig. 3, and Fig. 4) at seizure onset to visualize recruitment dynamics. PV-INs showed similar temporal recruitment patterns compared to PCs during seizures in *Scn1a*.PV-Cre mice (Fig. 2, Panel D). Similarly, VIP-INs showed a similar recruitment pattern compared to PCs during seizures in *Scn1a*.VIP-Cre mice (Fig. 4, Panel D). However, we found that SST-INs exhibit a distinct and early recruitment pattern in the preictal period compared to PCs as shown in *Scn1a*.SST-Cre mice (Fig. 3, Panel D). We further investigated recruitment dynamics by deriving the recruitment lags relative to seizure onset.

We compared the recruitment lags between each IN class (Fig. 5A). Linear mixed modeling with seizure number as a random factor was performed to calculate the mean, standard error,

and p-value of the lags of each IN subclass relative to seizure onset. The recruitment lags of each IN subclass were compared with seizure onset, which demonstrated no significant differences for PV-INs (−0.247 ± 0.879 s, $p > 0.05$) and VIP-INs (−1.895 ± 1.711 s, $p > 0.05$) but a significant difference for SST-INs (−3.237 ± 1.156 s, $p < 0.01$) when compared with seizure onset (at 0 s). The results confirm significant early recruitment of SST-INs relative to other cell types during temperature-induced seizures in *Scn1a*+/− mice.

We derived recruitment as the maximum d$F/F0$ value of each cell during seizure onset and compared this between the neuronal classes (Fig. 5B). Linear mixed modeling with seizure number as a random factor was performed to calculate group means, standard error, and p-value for the experiment. For the PV-IN dataset, the mean dF/F_0 of non-PV cells was 6.77 ± 0.40, and for PV-INs was 6.79 ± 1.20, which was not significantly different from each other ($p > 0.05$). For the SST-IN dataset, the mean dF/F_0 of non-SST cells was 5.32 ± 0.41, and for SST-INs was 4.97 ± 0.63, which was also not significantly different from each other ($p > 0.05$). However, for the VIP-IN dataset, the mean dF/F_0 of non-VIP cells was 4.69 ± 0.33, while for VIP-INs it was 2.89 ± 0.51 ($p < 0.001$). These results confirm that the magnitude of recruitment of PV-INs and SST-INs in response to seizures was similar to PCs as reported by 2P calcium imaging with GCaMP6f, while VIP-INs do not exhibit a similar maximal increase in dF/F_0.

The cellular resolution afforded by 2P imaging combined with the ability to label genetically defined subsets of cells facilitates unprecedented investigation into the cellular architecture of seizures. An example field of view (with cells color-coded based on lag relative to seizure onset) is shown in Fig. 6. The general observed pattern of seizure propagation is across the cortical surface, and, in general, INs are recruited along with neighboring putative excitatory PCs. However, this analysis revealed a prominent subset of SST-INs which are recruited independently, irrespective of what appears to be a traveling wave across the neocortex (highlighted in Fig. 6B).

4. Discussion

Here we discuss an experimental approach that facilitates *in vivo* 2P imaging of naturalistic seizures in an awake head-fixed preparation of an experimental mouse model of a prominent genetic epilepsy syndrome *in vivo.* This approach is combined with measures of behavior including running speed and pupilometry. Many experimental mouse models of genetic epilepsy may be challenging to study using *in vivo* 2P imaging either due to rare seizures (rendering it unlikely to capture a seizure during a standard recording session) or, on the other end of the spectrum, due to a severe epilepsy phenotype associated with early-onset seizures and mortality. Mouse models of acquired epilepsy such as the systemic pilocarpine or intrahippocampal kainate model of chronic acquired temporal lobe epilepsy after chemoconvulsant-induced status epilepticus may produce convulsive generalized tonic-clonic seizures. These are not compatible with prolonged stable imaging sessions in the head-fixed preparation. However, our approach could be applied towards imaging spontaneous seizures in *Scn1a*+/− mice (i.e., not provoked by temperature, although these occur on average once every 2 days [41]), temperature-induced seizures in other mouse models, or of spontaneous non-convulsive seizures – such as absence, myoclonic, or

infantile spasms – in other genetic models of epilepsy. As 2P imaging yields cellular-resolution and cell type-specific neural data, it can facilitate the investigation of cellular and circuit mechanisms of seizure generation, propagation, and termination [16,17,27], which remain central unresolved issues in the epilepsy field.

INs are hypothesized to play a central role in the pathophysiology of epilepsy. Data presented in this study shows a differential IN type-specific recruitment relative to seizure onset, with a prominent subset of SST-INs recruited seconds prior to seizure onset. This subset of SST-INs are also recruited in a spatiotemporal pattern that appears separate from the hypersynchronous traveling wave that generally characterizes seizure propagation across neocortex in this model.

However, the implications of this differential temporal recruitment for seizure initiation and propagation are not clear and require further investigation. Furthermore, the mechanism whereby SST-INs are seemingly recruited earlier than PCs and other IN subclasses is also unclear. It is possible that such early recruitment reflects impaired inhibition by VIP-INs, which themselves are known to prominently inhibit SST-INs and thereby subserve a "disinhibitory" role in cerebral cortex circuits. Prior work showed that the cellular dysfunction of PV-INs in *Scn1a*+/− mice was in fact transient, being restricted to early developmental time points [37]; the electrical activity of PV-INs was shown to be normal in *Scn1a*+/− mice *in vivo* using juxtacellular recordings in an anesthetized preparation [42], and our 2P imaging study showed normal activity levels of PV-INs in *Scn1a*+/− mice during quiet wakefulness *in vivo* [19]. However, VIP-INs also express Nav1.1 and exhibit impaired action potential generation in acute brain slices prepared from *Scn1a*+/− mice *in vitro*, yet this dysfunction persists at later developmental time points (as opposed to PV-INs) [38]. We also identified a marked decrease in VIP-IN maximal dF/F_0 here which could reflect cell subclass-specific differences in operation of the GCaMP6 reporter but could also be due to differences in cellular excitability. Future work combining manipulation of SST and VIP-INs in the preictal period and targeted electrophysiological recordings from these defined IN subclasses could further clarify these important issues.

The limitations of this approach are as follows. A main concern is that calcium indicators cannot distinguish between prolonged tonic firing vs. depolarization block. Most of the cells recruited by seizure continued to be active for an extended period (on the order of 10 seconds) beyond the time of seizure onset. This could be due to prolonged hypersynchronous discharge, transition to depolarization block, and/or could represent an artifact of the slow kinetics of the calcium indicators or some other source of intracellular calcium. We scrutinized the dF/F_0 traces and did find fluctuations in many putative excitatory PCs suggesting ongoing spiking, but generally did not observe this in INs, which could suggest depolarization block, or saturation of the calcium indicator. Other approaches such as combined imaging and *in vivo* patch-clamp recording, or *in vivo* voltage imaging [43], could potentially be used to address this issue.

Seizures are large-scale network phenomena, and our approach is limited to imaging of seizure propagation across a small (approximately 500 × 500 μm) area of the superficial neocortex rather than the region of seizure generation. Large-scale/"mesoscopic" imaging

approaches and advanced optics (such as lateral scanning, beam multiplexing, and objectives engineered to facilitate a large field of view) can capture a 2 × 2 or 3 × 3 cm region or more, including hundreds of thousands of neurons [18,37,38]. Modifications to the cranial window preparation, such as replacing the entire dorsal aspect of the skull with a transparent window [44,45], also facilitate large-scale imaging [46]. A combination of such approaches could achieve cellular-resolution imaging of excitatory and inhibitory INs across extended brain areas and at depth to potentially achieve simultaneous recording of seizure focus *and* propagation to provide truly novel views of the dynamic cellular and network architecture of seizures to fully capitalize on and apply the power and latest advances of 2P imaging to the study of seizures and epilepsy.

Acknowledgements

This work was supported by NIH NINDS F31 NS111803 to K.M.G., a Postdoctoral Fellowship Award from the Dravet Syndrome Foundation to A.S., and NIH NINDS K08 NS097633, NIH NINDS R01 NS110869, the Dana Foundation David Mahoney Neuroimaging Program research grant, and the Burroughs Wellcome Fund Career Award for Medical Scientists to E.M.G. We thank Xiaohong Zhang for technical support and the GENIE project and the Janelia Research Campus of the HHMI for distribution of GCaMP6 and 7.

References

[1]. Tremblay R, Lee S, Rudy B, GABAergic Interneurons in the Neocortex: From Cellular Properties to Circuits, Neuron. 91 (2016) 260–292. 10.1016/j.neuron.2016.06.033. [PubMed: 27477017]

[2]. Gouwens NW, Sorensen SA, Baftizadeh F, Budzillo A, Lee BR, Jarsky T, Alfiler L, Baker K, Barkan E, Berry K, Bertagnolli D, Bickley K, Bomben J, Braun T, Brouner K, Casper T, Crichton K, Daigle TL, Dalley R, de Frates RA, Dee N, Desta T, Lee SD, Dotson N, Egdorf T, Ellingwood L, Enstrom R, Esposito L, Farrell C, Feng D, Fong O, Gala R, Gamlin C, Gary A, Glandon A, Goldy J, Gorham M, Graybuck L, Gu H, Hadley K, Hawrylycz MJ, Henry AM, Hill DJ, Hupp M, Kebede S, Kim TK, Kim L, Kroll M, Lee C, Link KE, Mallory M, Mann R, Maxwell M, McGraw M, McMillen D, Mukora A, Ng L, Ng L, Ngo K, Nicovich PR, Oldre A, Park D, Peng H, Penn O, Pham T, Pom A, Popović Z, Potekhina L, Rajanbabu R, Ransford S, Reid D, Rimorin C, Robertson M, Ronellenfitch K, Ruiz A, Sandman D, Smith K, Sulc J, Sunkin SM, Szafer A, Tieu M, Torkelson A, Trinh J, Tung H, Wakeman W, Ward K, Williams G, Zhou Z, Ting JT, Arkhipov A, Sümbül U, Lein ES, Koch C, Yao Z, Tasic B, Berg J, Murphy GJ, Zeng H, Integrated Morphoelectric and Transcriptomic Classification of Cortical GABAergic Cells, Cell. 183 (2020) 935–953.e19. 10.1016/j.cell.2020.09.057. [PubMed: 33186530]

[3]. Lee S, Kruglikov I, Huang ZJ, Fishell G, Rudy B, A disinhibitory circuit mediates motor integration in the somatosensory cortex, Nat. Neurosci 16 (2013) 1662–1670. 10.1038/nn.3544. [PubMed: 24097044]

[4]. Pi HJ, Hangya B, Kvitsiani D, Sanders JI, Huang ZJ, Kepecs A, Cortical interneurons that specialize in disinhibitory control, Nature. 503 (2013) 521–524. 10.1038/nature12676. [PubMed: 24097352]

[5]. Pfeffer CK, Inhibitory Neurons: Vip Cells Hit the Brake on Inhibition, Curr. Biol 24 (2014) R18–R20. 10.1016/j.cub.2013.11.001. [PubMed: 24405670]

[6]. Guet-McCreight A, Skinner FK, Topolnik L, Common Principles in Functional Organization of VIP/Calretinin Cell-Driven Disinhibitory Circuits Across Cortical Areas, Front. Neural Circuits 14 (2020). 10.3389/fncir.2020.00032.

[7]. Bartos M, Vida I, Jonas P, Synaptic mechanisms of synchronized gamma oscillations in inhibitory interneuron networks, Nat. Rev. Neurosci 8 (2007) 45–56. 10.1038/nrn2044. [PubMed: 17180162]

[8]. Sohal VS, Zhang F, Yizhar O, Deisseroth K, Parvalbumin neurons and gamma rhythms enhance cortical circuit performance, Nature. 459 (2009) 698–702. 10.1038/nature07991. [PubMed: 19396159]

[9]. Cardin JA, Carlén M, Meletis K, Knoblich U, Zhang F, Deisseroth K, Tsai LH, Moore CI, Driving fast-spiking cells induces gamma rhythm and controls sensory responses, Nature. 459 (2009) 663–667. 10.1038/nature08002. [PubMed: 19396156]

[10]. Jiang X, Lachance M, Rossignol E, Involvement of cortical fast-spiking parvalbumin-positive basket cells in epilepsy, in: Prog. Brain Res, Elsevier B.V., 2016: pp. 81–126. 10.1016/bs.pbr.2016.04.012.

[11]. Schwartzkroin PA, Prince DA, Changes in excitatory and inhibitory synaptic potentials leading to epileptogenic activity, Brain Res. 183 (1980) 61–77. 10.1016/0006-8993(80)90119-5. [PubMed: 6244050]

[12]. Prince DA, Connors BW, Mechanisms of epileptogenesis in cortical structures, Ann. Neurol 16 (1984) S59–S64. 10.1002/ana.410160710. [PubMed: 6095743]

[13]. Ziburkus J, Cressman JR, Barreto E, Schiff SJ, Interneuron and pyramidal cell interplay during in vitro seizure-like events, J. Neurophysiol 95 (2006) 3948–3954. 10.1152/jn.01378.2005. [PubMed: 16554499]

[14]. Avoli M, de Curtis M, GABAergic synchronization in the limbic system and its role in the generation of epileptiform activity, Prog. Neurobiol 95 (2011) 104–132. 10.1016/j.pneurobio.2011.07.003. [PubMed: 21802488]

[15]. Cope DW, Di Giovanni G, Fyson SJ, Orbán G, Errington AC, Lrincz ML, Gould TM, Carter DA, Crunelli V, Enhanced tonic GABA A inhibition in typical absence epilepsy, Nat. Med 15 (2009) 1392–1398. 10.1038/nm.2058. [PubMed: 19966779]

[16]. Wenzel M, Hamm JP, Peterka DS, Yuste R, Reliable and Elastic Propagation of Cortical Seizures In Vivo, Cell Rep. 19 (2017) 2681–2693. 10.1016/j.celrep.2017.05.090. [PubMed: 28658617]

[17]. Wenzel M, Hamm JP, Peterka DS, Yuste R, Acute Focal Seizures Start As Local Synchronizations of Neuronal Ensembles, J. Neurosci 39 (2019) 8562–8575. 10.1523/JNEUROSCI.3176-18.2019. [PubMed: 31427393]

[18]. Aeed F, Shnitzer T, Talmon R, Schiller Y, Layer- and Cell-Specific Recruitment Dynamics during Epileptic Seizures In Vivo, Ann. Neurol 87 (2020) 97–115. 10.1002/ana.25628. [PubMed: 31657482]

[19]. Tran CH, Vaiana M, Nakuci J, Somarowthu A, Goff KM, Goldstein N, Murthy P, Muldoon SF, Goldberg EM, Interneuron Desynchronization Precedes Seizures in a Mouse Model of Dravet Syndrome, J. Neurosci 40 (2020) 2764–2775. 10.1523/JNEUROSCI.2370-19.2020. [PubMed: 32102923]

[20]. Buzsáki G, Anastassiou CA, Koch C, The origin of extracellular fields and currents-EEG, ECoG, LFP and spikes, Nat. Rev. Neurosci 13 (2012) 407–420. 10.1038/nrn3241. [PubMed: 22595786]

[21]. Schevon CA, Weiss SA, McKhann G, Goodman RR, Yuste R, Emerson RG, Trevelyan AJ, Evidence of an inhibitory restraint of seizure activity in humans, Nat. Commun 3 (2012) 1–11. 10.1038/ncomms2056.

[22]. Smith EH, Liou JY, Davis TS, Merricks EM, Kellis SS, Weiss SA, Greger B, House PA, McKhann GM, Goodman RR, Emerson RG, Bateman LM, Trevelyan AJ, Schevon CA, The ictal wavefront is the spatiotemporal source of discharges during spontaneous human seizures, Nat. Commun 7 (2016) 1–12. 10.1038/ncomms11098.

[23]. Ahmed OJ, John TT, Sudhakar SK, Brennan EK, Lorenzo Gonzalez A, Naftulin JS, Eskandar E, Madsen JR, Cosgrove R, Blum AS, Stevenson Potter N, Mashour GA, Two modes of inhibitory neuronal shutdown distinctly amplify seizures in humans, MedRxiv. 8 (2020) 2020.10.09.20204206. 10.1101/2020.10.09.20204206.

[24]. Jun JJ, Steinmetz NA, Siegle JH, Denman DJ, Bauza M, Barbarits B, Lee AK, Anastassiou CA, Andrei A, Aydin Ç, Barbic M, Blanche TJ, Bonin V, Couto J, Dutta B, Gratiy SL, Gutnisky DA, Häusser M, Karsh B, Ledochowitsch P, Lopez CM, Mitelut C, Musa S, Okun M, Pachitariu M, Putzeys J, Rich PD, Rossant C, Sun WL, Svoboda K, Carandini M, Harris KD, Koch C, O'Keefe J, Harris TD, Fully integrated silicon probes for high-density recording of neural activity, Nature. 551 (2017) 232–236. 10.1038/nature24636. [PubMed: 29120427]

[25]. Steinmetz NA, Koch C, Harris KD, Carandini M, Challenges and opportunities for large-scale electrophysiology with Neuropixels probes, Curr. Opin. Neurobiol 50 (2018) 92–100. 10.1016/j.conb.2018.01.009. [PubMed: 29444488]

[26]. Rossi LF, Kullmann DM, Wykes RC, The enlightened brain: Novel imaging methods focus on epileptic networks at multiple scales, Front. Cell. Neurosci 12 (2018). 10.3389/fncel.2018.00082.

[27]. Meyer J, Maheshwari A, Noebels J, Smirnakis S, Asynchronous suppression of visual cortex during absence seizures in stargazer mice, Nat. Commun 9 (2018) 1–9. 10.1038/s41467-018-04349-8. [PubMed: 29317637]

[28]. Muldoon SF, Villette V, Tressard T, Malvache A, Reichinnek S, Bartolomei F, Cossart R, GABAergic inhibition shapes interictal dynamics in awake epileptic mice, Brain. 138 (2015) 2875–2890. 10.1093/brain/awv227. [PubMed: 26280596]

[29]. Ewell LA, Déjà Vu: Same pattern of neuron activation from seizure to seizure, only the timing changes, Epilepsy Curr. 18 (2018) 131–132. 10.5698/1535-7597.18.2.131. [PubMed: 29643754]

[30]. Andermann ML, Gilfoy NB, Goldey GJ, Sachdev RNS, Wölfel M, McCormick DA, Reid RC, Levene MJ, Chronic Cellular Imaging of Entire Cortical Columns in Awake Mice Using Microprisms, Neuron. 80 (2013) 900–913. 10.1016/j.neuron.2013.07.052. [PubMed: 24139817]

[31]. Wu YW, Sullivan J, McDaniel SS, Meisler MH, Walsh EM, Li SX, Kuzniewicz MW, Incidence of dravet syndrome in a US population, Pediatrics. 136 (2015) e1310–e1315. 10.1542/peds.2015-1807. [PubMed: 26438699]

[32]. Ito S, Ogiwara I, Yamada K, Miyamoto H, Hensch TK, Osawa M, Yamakawa K, Mouse with Nav1.1 haploinsufficiency, a model for Dravet syndrome, exhibits lowered sociability and learning impairment, Neurobiol. Dis 49 (2013) 29–40. 10.1016/j.nbd.2012.08.003. [PubMed: 22986304]

[33]. Tai C, Abe Y, Westenbroek RE, Scheuer T, Catterall WA, Impaired excitability of somatostatin- and parvalbumin-expressing cortical interneurons in a mouse model of Dravet syndrome, Proc. Natl. Acad. Sci. U. S. A 111 (2014). 10.1073/pnas.1411131111.

[34]. Sun Y, Paşca SP, Portmann T, Goold C, Worringer KA, Guan W, Chan KC, Gai H, Vogt D, Chen YJJ, Mao R, Chan K, Rubenstein JLR, Madison DV, Hallmayer J, Froehlich-Santino WM, Bernstein JA, Dolmetsch RE, A deleterious Nav1.1 mutation selectively impairs telencephalic inhibitory neurons derived from Dravet Syndrome patients, Elife. 5 (2016). 10.7554/eLife.13073.

[35]. Yu FH, Mantegazza M, Westenbroek RE, Robbins CA, Kalume F, Burton KA, Spain WJ, McKnight GS, Scheuer T, Catterall WA, Reduced sodium current in GABAergic interneurons in a mouse model of severe myoclonic epilepsy in infancy, Nat. Neurosci 9 (2006) 1142–1149. 10.1038/nn1754. [PubMed: 16921370]

[36]. Ogiwara I, Miyamoto H, Morita N, Atapour N, Mazaki E, Inoue I, Takeuchi T, Itohara S, Yanagawa Y, Obata K, Furuichi T, Hensch TK, Yamakawa K, Nav1.1 localizes to axons of parvalbumin-positive inhibitory interneurons: A circuit basis for epileptic seizures in mice carrying an Scn1a gene mutation, J. Neurosci 27 (2007) 5903–5914. 10.1523/JNEUROSCI.5270-06.2007. [PubMed: 17537961]

[37]. Favero M, Sotuyo NP, Lopez E, Kearney JA, Goldberg EM, A transient developmental window of fast-spiking interneuron dysfunction in a mouse model of dravet syndrome, J. Neurosci 38 (2018) 7912–7927. 10.1523/JNEUROSCI.0193-18.2018. [PubMed: 30104343]

[38]. Goff KM, Goldberg EM, Vasoactive intestinal peptide-expressing interneurons are impaired in a mouse model of dravet syndrome, Elife. 8 (2019). 10.7554/eLife.46846.

[39]. Pachitariu M, Stringer C, Dipoppa M, Schröder S, Rossi LF, Dalgleish H, Carandini M, Harris K, Suite2p: beyond 10,000 neurons with standard two-photon microscopy, BioRxiv. (2016) 061507. 10.1101/061507.

[40]. Mathis A, Mamidanna P, Cury KM, Abe T, Murthy VN, Mathis MW, Bethge M, DeepLabCut: markerless pose estimation of user-defined body parts with deep learning, Nat. Neurosci 21 (2018) 1281–1289. 10.1038/s41593-018-0209-y. [PubMed: 30127430]

[41]. Mistry AM, Thompson CH, Miller AR, Vanoye CG, George AL, Kearney JA, Strain-and age-dependent hippocampal neuron sodium currents correlate with epilepsy severity in Dravet syndrome mice, (2014). 10.1016/j.nbd.2014.01.006.

[42]. De Stasi AM, Farisello P, Marcon I, Cavallari S, Forli A, Vecchia D, Losi G, Mantegazza M, Panzeri S, Carmignoto G, Bacci A, Fellin T, Unaltered Network Activity and Interneuronal Firing during Spontaneous Cortical Dynamics in Vivo in a Mouse Model of Severe Myoclonic

Epilepsy of Infancy, Cereb. Cortex 26 (2016) 1778–1794. 10.1093/cercor/bhw002. [PubMed: 26819275]

[43]. Piatkevich KD, Bensussen S, an Tseng H, Shroff SN, Lopez-Huerta VG, Park D, Jung EE, Shemesh OA, Straub C, Gritton HJ, Romano MF, Costa E, Sabatini BL, Fu Z, Boyden ES, Han X, Population imaging of neural activity in awake behaving mice in multiple brain regions, BioRxiv. (2019) 616094. 10.1101/616094.

[44]. Sofroniew NJ, Flickinger D, King J, Svoboda K, A large field of view two-photon mesoscope with subcellular resolution for in vivo imaging, Elife. 5 (2016). 10.7554/eLife.14472.

[45]. Stirman JN, Smith IT, Kudenov MW, Smith SL, Wide field-of-view, multi-region, two-photon imaging of neuronal activity in the mammalian brain, Nat. Biotechnol 34 (2016) 857–862. 10.1038/nbt.3594. [PubMed: 27347754]

[46]. Kim TH, Zhang Y, Lecoq J, Jung JC, Li J, Zeng H, Niell CM, Schnitzer MJ, Long-Term Optical Access to an Estimated One Million Neurons in the Live Mouse Cortex, Cell Rep. 17 (2016) 3385–3394. 10.1016/j.celrep.2016.12.004. [PubMed: 28009304]

Highlights

- We review recent work applying two-photon calcium imaging to study mechanisms of seizure generation and propagation in awake, head-fixed mice.
- Highlighted are recent findings in an experimental mouse model of Dravet syndrome (*Scn1a*+/− mice).
- We present new data demonstrating differential recruitment of cerebral cortex GABAergic interneurons during seizure showing early recruitment of somatostatin interneurons (SST-INs).

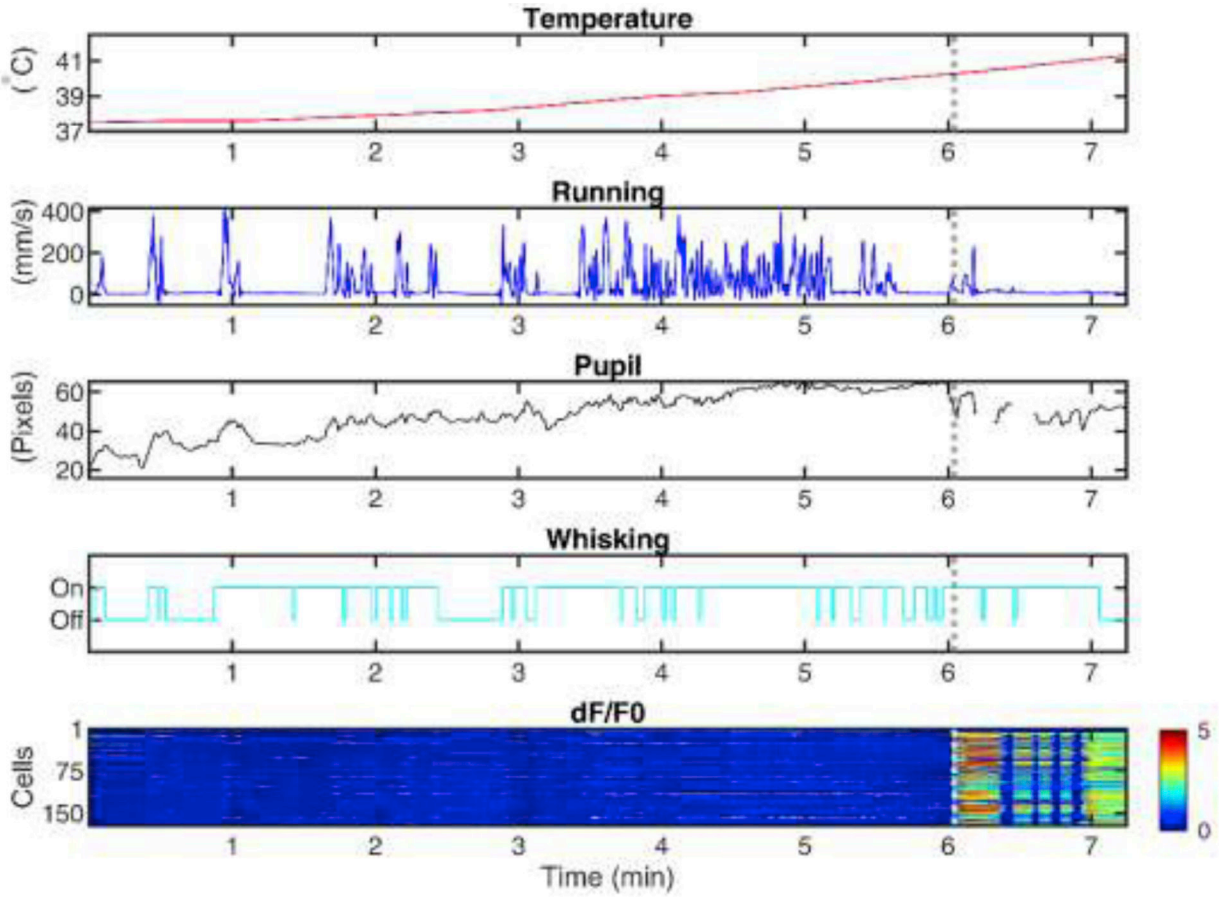

Fig. 1.

Acquisition of multimodal behavioral and 2P imaging data during seizures in awake, behaving, head-fixed experimental mouse models of epilepsy.

Shown is an example of behavioral and neural traces recorded in one session while the body temperature is elevated continuously. (A) Body temperature in degrees C. (B) Running speed in mm/s. (C) Pupil diameter in pixels. (D) Whisking (upward deflection, on; downward deflection, off). (E) Heatmap showing the change in fluorescence of each cell (y-axis) over time (x-axis). The dotted white line shows seizure onset.

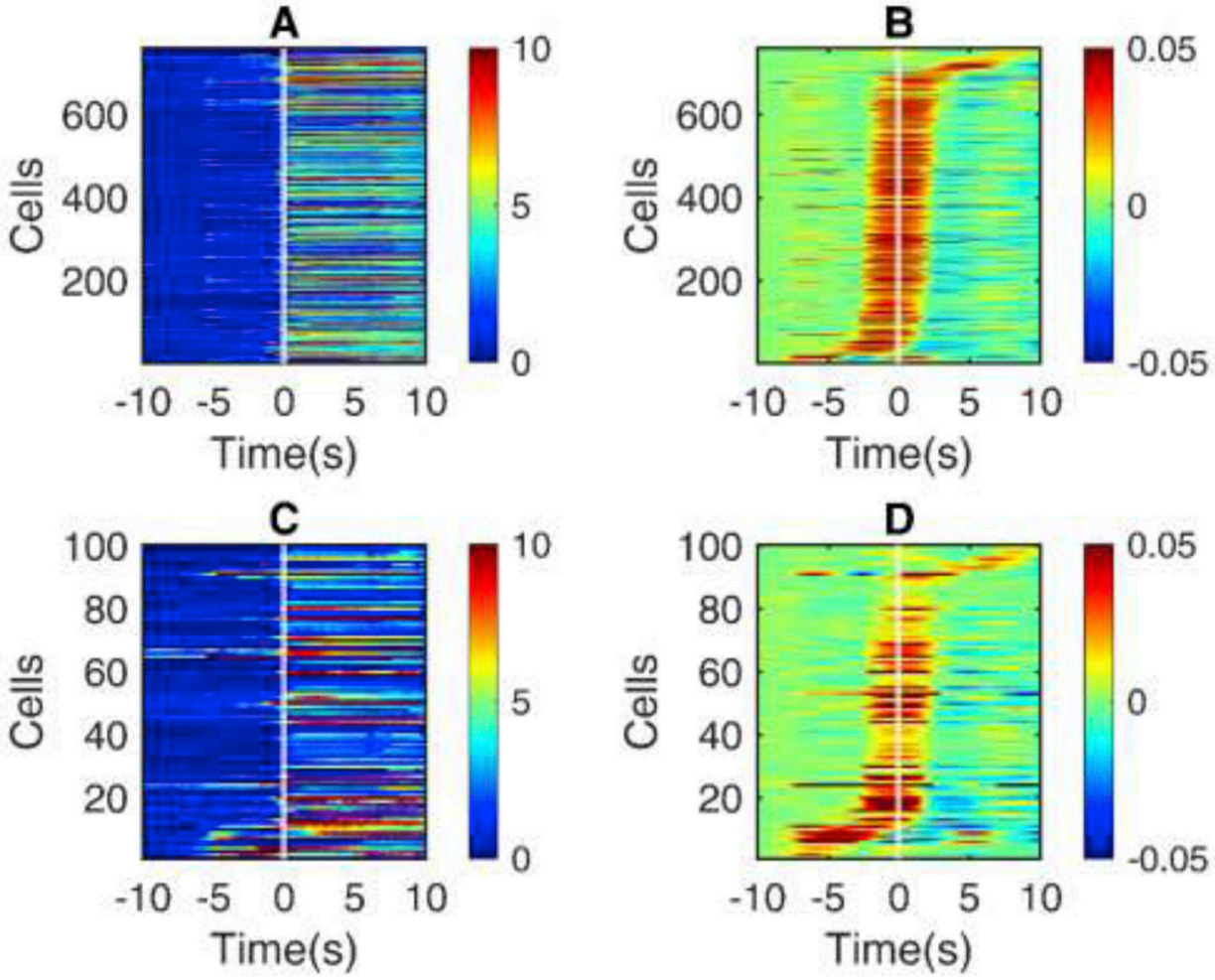

Fig. 2.

The activity of PV-INs prior to seizure onset.

Shown is the seizure onset window for all seizures in *Scn1a*.PV-Cre mice (n = 6). (A) Heatmap of change in fluorescence (dF/F_0) traces of non-PV cells. (B) Slope, calculated as the difference between adjacent fluorescence values for each non-PV cell. (C) dF/F_0 traces of PV-IN. (D) Slopes of dF/F0 traces in PV cells. All the cells are sorted in the order of recruitment lags.

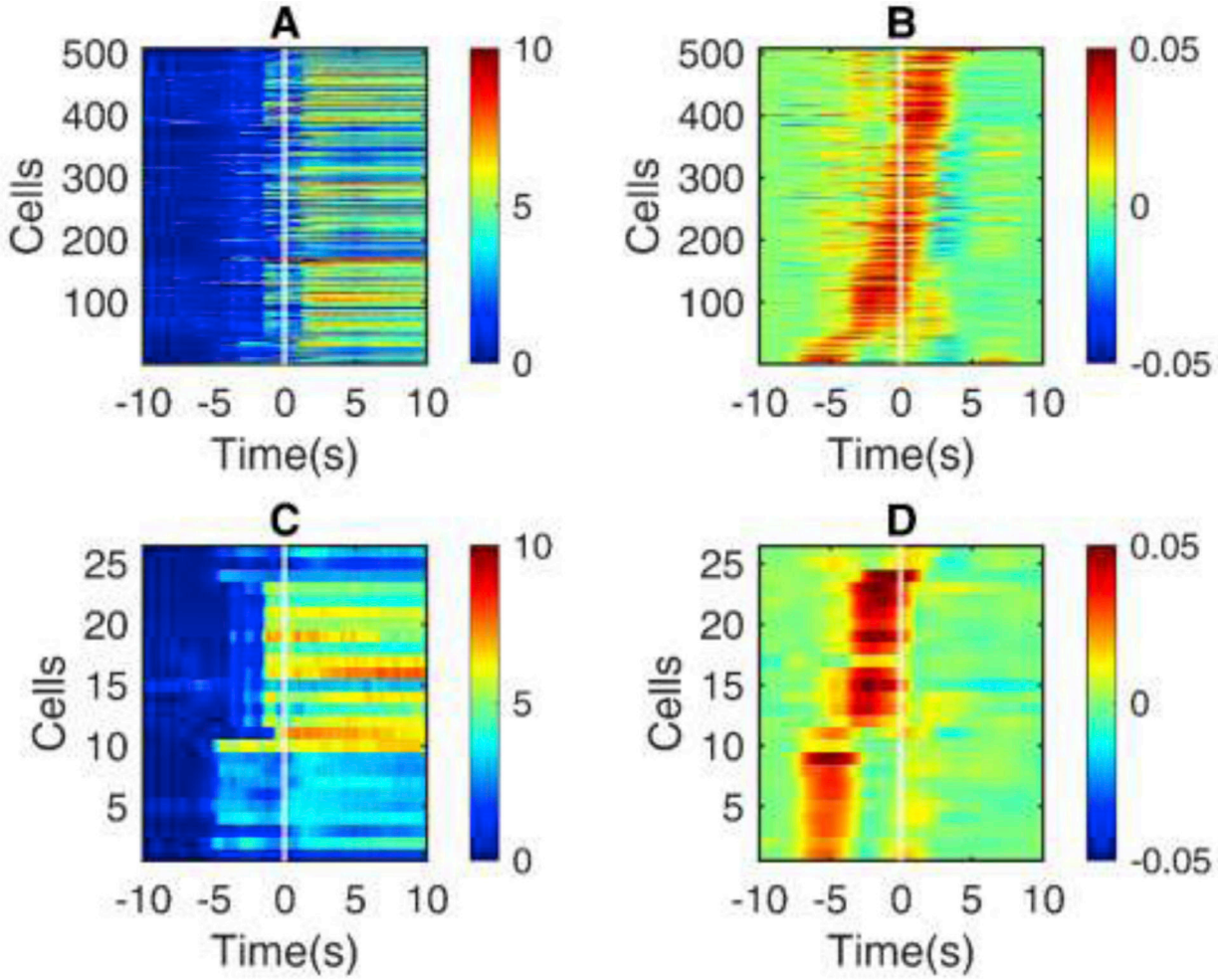

Fig. 3.

The activity of SST-INs prior to seizure onset.

Shown is the seizure onset window for all seizures in *Scn1a*.SST-Cre mice (n = 2). (A Heatmap of change in fluorescence (dF/F_0) traces of non-SST cells, similar to Fig. 2A. (B) Slope for each non-SST cell, as in Fig. 2B. (C) dF/F_0 traces of SST-INs. (C) Slopes of dF/F0 traces in SST-INs. All the cells are sorted in the order of recruitment lags.

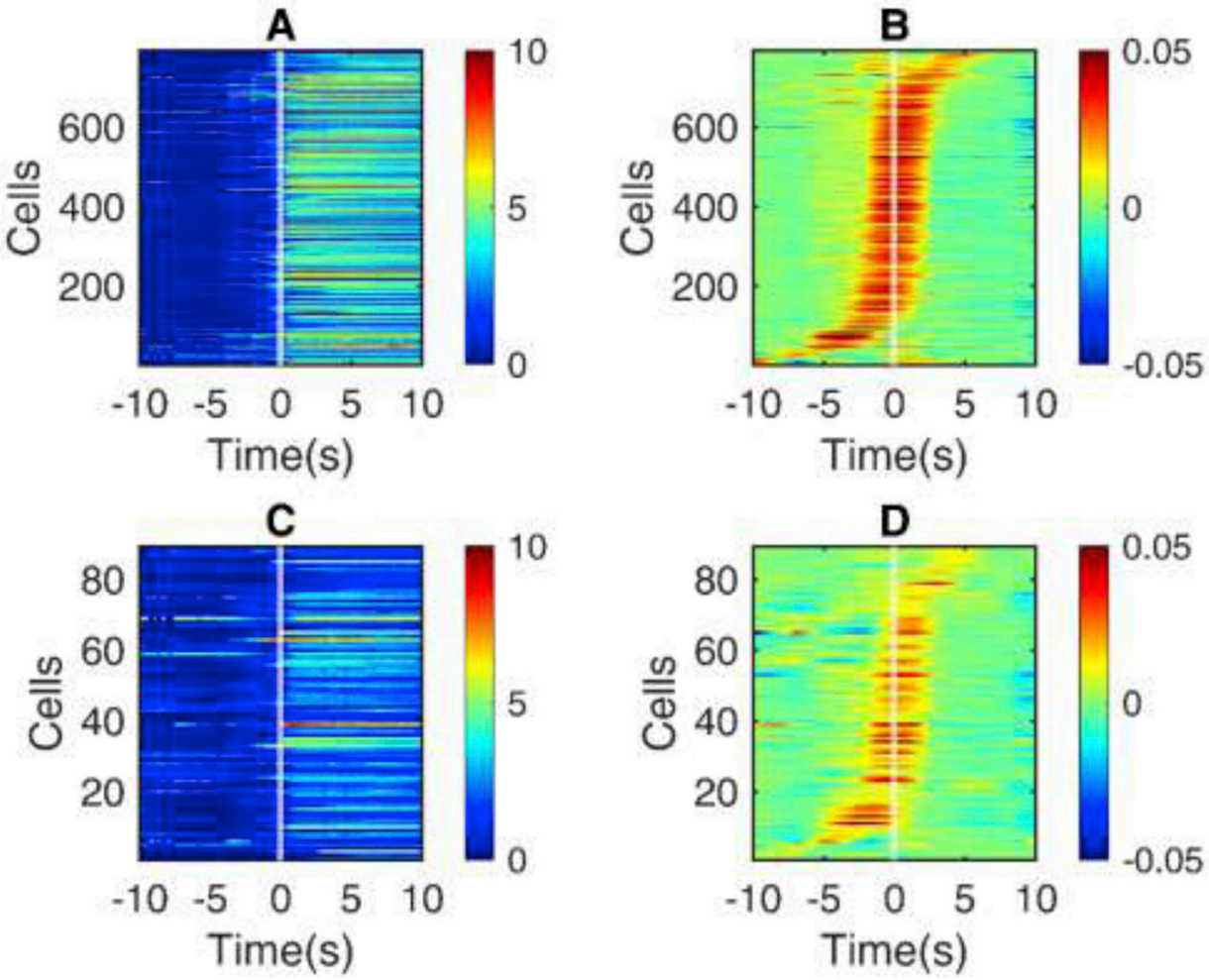

Fig. 4.

The activity of VIP-INs prior to seizure onset.

Shown is the seizure onset window for all seizures in *Scn1a*.VIP-Cre mice (n = 4). (A) Heatmap of change in fluorescence (dF/F_0) traces of non-VIP cells as in Fig. 2A, 3A. (B) Slope for each non-VIP cell as in Fig. 2B, 3B. (C) dF/F0 traces of VIP-INs. (D) Slopes of dF/F0 traces in VIP-INs. All the cells are sorted in the order of recruitment lags.

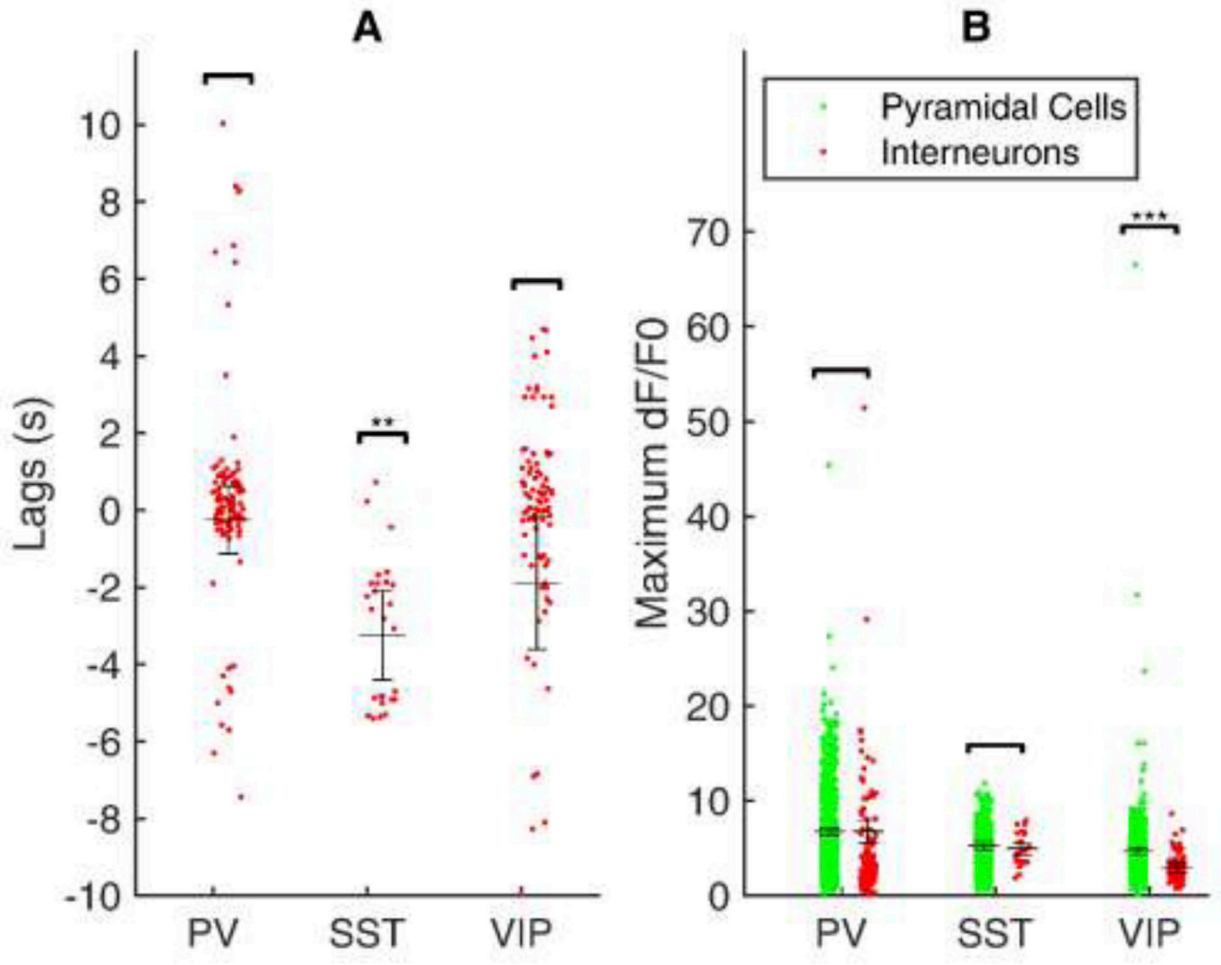

Fig. 5:

Recruitment lags and response of distinct subclasses of interneurons during seizure.

(A) Individual points shows the lag of each cell corresponding to the seizure onset. SST INs alone have shown a significant difference compared to seizure onset ($p < 0.01$). (B) Individual points shows maximum fluorescence (dF/F_0) of each cell. A significant difference is shown for VIP cells alone ($p < 0.001$). The horizontal line depicts the mean, and the error bar reports the standard error. Significance is tested with mixed modeling considering each seizure as a random factor.

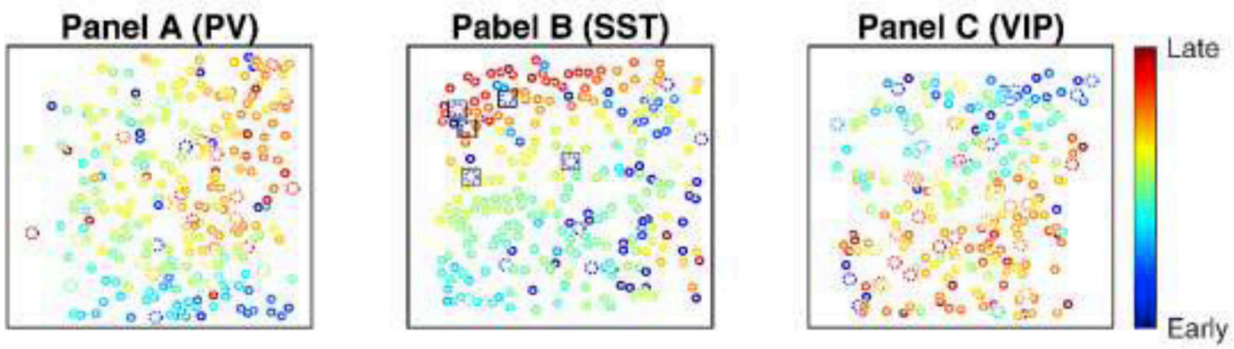

Fig. 6.

Depiction of spatiotemporal recruitment of defined subclasses of cells during seizure propagation.

Cells are color coded on the scale of recruitment lags. (A) An example field of view of a seizure in an *Scn1a*.PV-Cre mouse. (B) An example field of view of a seizure in an *Scn1a*.SST-Cre mouse. (C) An example field of view of a seizure in an *Scn1a*.VIP-Cre mouse. Interneurons are indicated by larger cells with dotted outlines, while all other circles are putative pyramidal cells. Dotted cells surrounded by squares show the SST-INs that are recruited early (not as a part of the travelling wave). Heat maps indicate early (*blue*) to late (*red*) recruitment during seizure.